

Aceno[2,1,3]thiadiazoles for Field-Effect Transistors: Synthesis and Crystal Packing

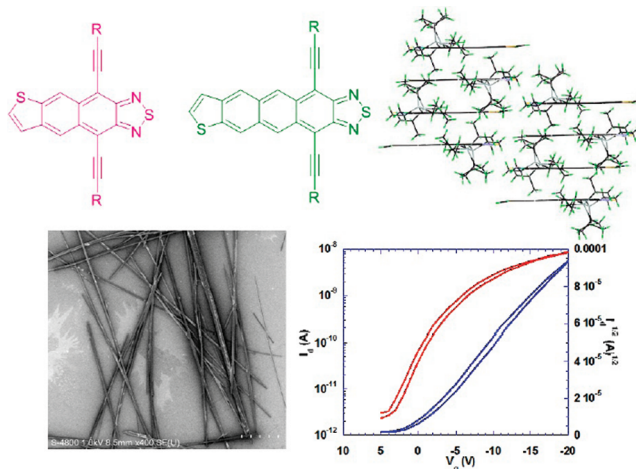
Ting Lei, Yan Zhou, Chu-Yang Cheng, Yue Cao, Yang Peng, Jiang Bian, and Jian Pei*

Beijing National Laboratory for Molecular Sciences, the Key Laboratory of Bioorganic Chemistry and Molecular Engineering of the Ministry of Education, College of Chemistry and Molecular Engineering, Peking University, Beijing 100871, China

jianpei@pku.edu.cn

Received March 21, 2011

ABSTRACT



An efficient synthetic approach to a series of aceno[2,1,3]thiadiazole derivatives is described. 2-TIPS and 2-TES molecules exhibited different crystal packings, and 2-TIPS show good device performances with hole mobility up to $0.4 \text{ cm}^2 \text{ V}^{-1} \text{ s}^{-1}$ and an average mobility of $0.15 \text{ cm}^2 \text{ V}^{-1} \text{ s}^{-1}$ as the active material for organic field-effect transistors. All of the results demonstrate these aceno[2,1,3]thiadiazole derivatives as promising materials for optoelectronic devices.

Oligoacenes are among the most important families of organic semiconductors because of their interesting electronic properties for organic field-effect transistors (OFETs) and organic photovoltaics (OPVs).¹ Recently, considerable investigations of the synthesis, functionalization,

and device performances of oligoacenes show their abundance of structure diversity and fascinating electronic properties.^{1–3} Figure 1 shows five typical pentacene derivatives, electron-rich tetraceno[2,3-*b*]thiophene (**Thio**) and electron-deficient tetraceno[2,3-*c*][1,2,5]thiadiazole (**Thia**), 1,2,3,4-tetrachloropentacene (**Chlo**), and 1,2,3,4-tetrafluoropentacene (**Fluo**). The syntheses and device performances of **Thio**, **Chlo**, and **Fluo** were widely investigated by Bao and Anthony et al.^{1,2} However, the synthetic approach to aceno[2,1,3]thiadiazoles (**Thia**) and their OFET performances have not yet been reported because of the complexity of the synthesis and the characterization.⁴

(1) (a) Anthony, J. E. *Angew. Chem., Int. Ed.* **2008**, *47*, 452. (b) Anthony, J. E. *Chem. Rev.* **2006**, *106*, 5028.

(2) (a) Tang, M. L.; Reichardt, A. D.; Wei, P.; Bao, Z. *J. Am. Chem. Soc.* **2009**, *131*, 5264. (b) Tang, M. L.; Oh, J. H.; Reichardt, A. D.; Bao, Z. *J. Am. Chem. Soc.* **2009**, *131*, 3733. (c) Tang, M. L.; Reichardt, A. D.; Miyaki, N.; Stoltenberg, R. M.; Bao, Z. *J. Am. Chem. Soc.* **2008**, *130*, 6064. (d) Tang, M. L.; Okamoto, T.; Bao, Z. *N. J. Am. Chem. Soc.* **2006**, *128*, 16002.

(3) (a) Miao, Q.; Chi, X.; Xiao, S.; Zeis, R.; Lefenfeld, M.; Siegrist, T.; Michael Steigerwald, L.; Nuckolls, C. *J. Am. Chem. Soc.* **2006**, *128*, 1340. (b) Miao, Q.; Lefenfeld, M.; Nguyen, T.-Q.; Siegrist, T.; Kloc, C.; Nuckolls, C. *Adv. Mater.* **2005**, *17*, 407. (c) Miao, Q.; Nguyen, T. Q.; Someya, T.; Blanchet, G. B.; Nuckolls, C. *J. Am. Chem. Soc.* **2003**, *125*, 10284.

(4) Appleton, A. L.; Miao, S.; Brombosz, S. M.; Berger, N. J.; Barlow, S.; Marder, S. R.; Lawrence, B. M.; Hardcastle, K. I.; Bunn, U. H. F. *Org. Lett.* **2009**, *11*, 5222.

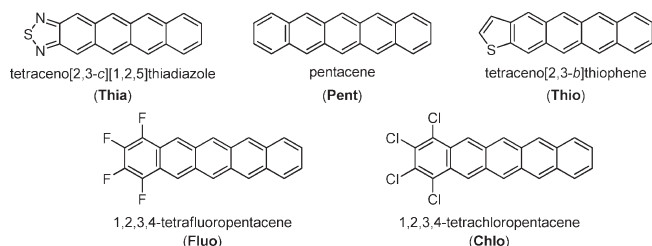


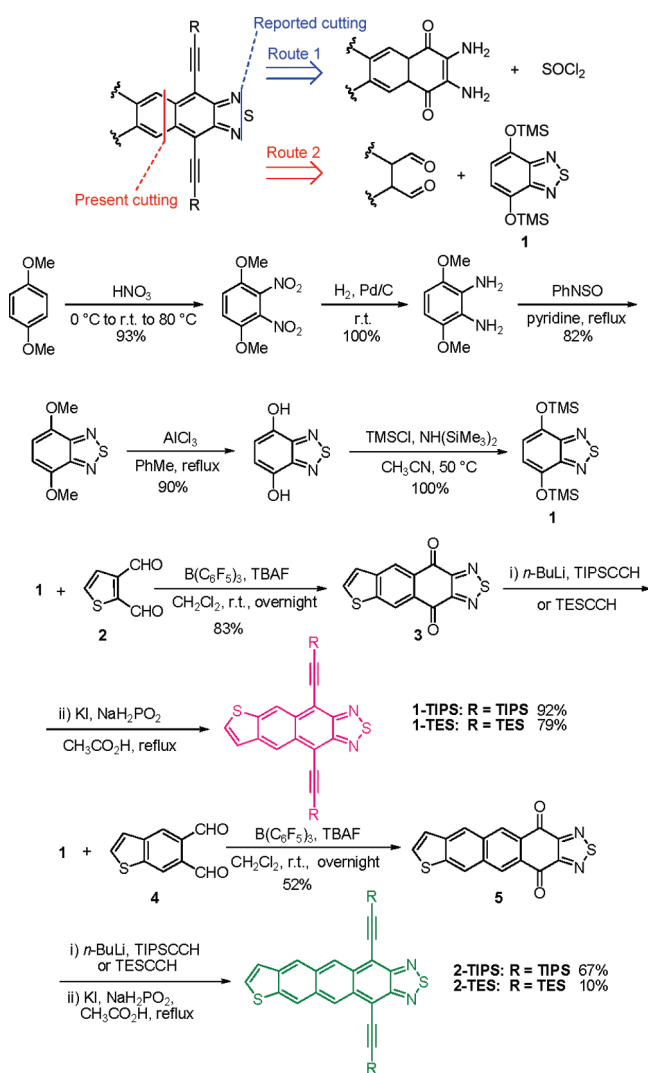
Figure 1. Five typical pentacene derivatives compared in discussion.

To understand the electronic properties of the aceno[2,1,3]thiadiazoles, the investigation of density functional theory (DFT) calculations for these five model oligoacene derivatives is summarized in Table S1 (Supporting Information). The calculations showed that compound **Thia** exhibited the lowest LUMO levels and the smallest bandgap among these five compounds, which might be attributed to its quinone form of electronic structure. Interestingly, aceno[2,1,3]thiadiazole derivatives also had the lowest positive charge transport reorganization energy. Therefore, it is believed that aceno[2,1,3]thiadiazole derivatives might show very promising charge transport properties as organic semiconducting materials.

Herein, we present a facile synthetic route and characterization of four aceno[2,1,3]thiadiazole derivatives for OFETs. The investigations demonstrate that these molecules easily self-assemble into single crystal nano/micro-wires (NWs/MWs) through π - π stacking. The crystal structures of **2-TIPS** and **2-TES** show different crystal packing compared to the reported pentacene counterparts. Finally, these MWs are employed as the active materials to directly fabricate OFET devices by solution process. The good performance with a hole mobility up to $0.4 \text{ cm}^2 \text{ V}^{-1} \text{ s}^{-1}$ is achieved from **2-TIPS**, which is quite high among the donor-acceptor pentacene derivatives.²

Scheme 1 presents two synthetic approaches to aceno[2,1,3]thiadiazole derivatives. Route 1 is ineffective for the construction of the aceno[2,1,3]thiadiazole skeleton fused with five or more rings because of the synthetic difficulty of some synthons.⁴ Herein, we adopted a Mukaiyama aldol reaction to synthesize larger acenes as shown in route 2. Synthon **1** was synthesized from commercial available 1,4-dimethoxybenzene in ten gram scales with very high yields as illustrated in Scheme 1. The Mukaiyama aldol reaction between **1** and thiophene-2,3-dicarbaldehyde were employed to afford quinone **3**, which was directly used in the next step after filtration and washing. An alkylation reaction of **3** with a mixture of *n*-BuLi and TIPSCCH or TESCCH following by a reduction with NaH_2PO_2 afforded the desired **1-TIPS** or **1-TES**. Following the same procedure, we also obtained **2-TIPS** and **2-TES** in good yields. We introduced triisopropylsilyl (TIPS) or triethylsilyl (TES) substituted acetylene units to enhance the solubility of the molecules and further ensure their good crystal packing.¹ Such a synthetic approach to aceno[2,1,3]thiadiazole

Scheme 1. Synthesis of Aceno[2,1,3]thiadiazole Derivatives Using a Mukaiyama Aldol Reaction



derivatives is widely applicable because many 1,2-dicarbaldehyde compounds are available to replace thiophene-2,3-dicarbaldehyde. These four molecules showed good solubility in common solvents, so it provided us convenience to purify and characterize their structures through ^1H and ^{13}C NMR and MS. The thermal decomposition temperature of $350 \text{ }^\circ\text{C}$ under nitrogen atmosphere revealed a good thermal stability of these four oligoacene derivatives.

The photophysical and the electrochemical properties of these four aceno[2,1,3]thiadiazoles were investigated in detail and summarized in Table S2 (Supporting Information). The absorption features of **1-TIPS** and **1-TES** peaked at 611 nm with an onset at 650 nm; however, **2-TIPS** and **2-TES** displayed absorption maximum λ_{max} at 730 nm with an onset at 810 nm, which showed obvious red-shift relative to **1-TIPS** and **1-TES** due to the increase of the effective conjugation length. The cyclic voltammetry (CV) measurement showed that **1-TIPS** and **1-TES** had HOMO/LUMO levels at $-5.67/-3.65 \text{ eV}$ with a bandgap of 2.02 eV, and **2-TIPS** and **2-TES** had HOMO/LUMO

levels at $-5.42/-3.78$ eV with a bandgap of 1.64 eV. Compared to **Chlo** (HOMO/LUMO: $-5.38/-3.45$ eV)^{2b} and **Fluo** (HOMO/LUMO: $-5.39/-3.35$ eV)^{2c} counterparts, the absorption bands of these molecules were much more red-shifted, which can be attributed to the much lowered LUMO levels induced by the [2,1,3]thiadiazole unit. Computational results indicated that the HOMO levels of these aceno[2,1,3]thiadiazoles were located on sulfur atom of the thiophene ring and their LUMO levels are located on the sulfur atom of the thiadiazole unit. Therefore, these molecules are typical donor–acceptor systems Figure S3 (Supporting Information).

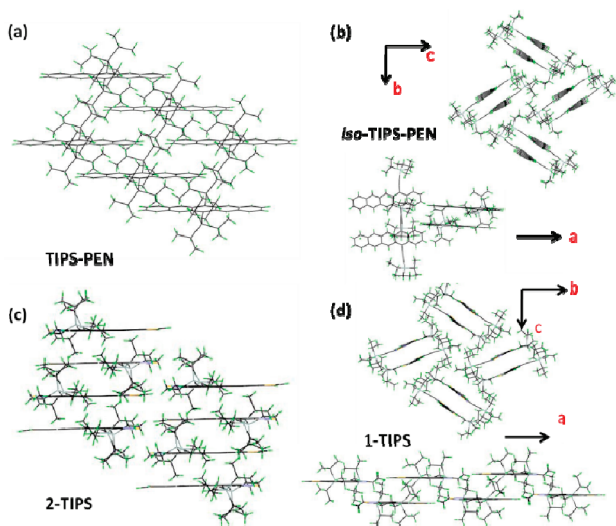


Figure 2. Single-crystal structure and packing of (a) **TIPS-PEN**, (b) **iso-TIPS-PEN**, (c) **1-TIPS**, and (d) **2-TIPS**.

The obtained single crystals of **1-TIPS**, **2-TIPS**, and **2-TES** exhibited unconventional crystal packing compared with other pentacene derivatives. **TIPS-PEN** and its derivatives always had well-ordered two-dimensional crystal packing (Figure 2a).^{1,2} **Iso-TIPS-PEN**, whose 5,14 positions were substituted with TIPS-acetylenyls, showed a two-pair herringbone packing (Figure 2b).⁵ However, **2-TIPS** and **2-TES** did not follow such packing models, which formed unconventional one-dimensional column packing (Figure 2c and Figure S6, Supporting Information). For **2-TIPS** and **2-TES**, in one column, the molecules were packed head-to-tail to form a long column, and the columns were packed together to form the crystals. Inside the column, both **2-TIPS** and **2-TES** exhibited good π – π stacking with a distance about 3.42 and 3.37 Å, respectively, both of which were smaller than that of **TIPS-PEN** (3.47 Å).⁵ The reduced packing distance might be caused by the strong donor–acceptor interactions. However, as shown in Figure 2d, the crystal structure of **1-TIPS** was very similar to that of **iso-TIPS-PEN**; such two-pair herringbone packing makes the molecule

(5) Anthony, J. E.; Brooks, J. S.; Eaton, D. L.; Parkin, S. R. *J. Am. Chem. Soc.* **2001**, *123*, 9482.

unsuitable for charge transport because of the lack of a long-distance charge-transporting channel.⁶

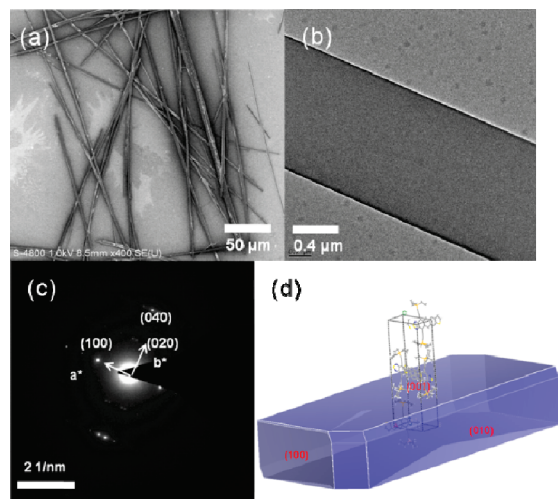


Figure 3. (a) SEM image, (b) TEM image, (c) electron diffraction pattern of **2-TES**, and (d) the theoretically predicted crystal habit using BFDH method.

Organic single crystal nano/microwires (NWs/MWs) have shown promising applications in the fabrication of high performance OFETs.^{7,8} Recently, the large-area alignment of solution processed nanowires is realized by Bao and co-workers through filtration and transfer method.⁹ Single crystal MWs of **2-TIPS** and **2-TES** were grown by a phase transfer procedure of injecting methanol into their CH_2Cl_2 (DCM) solution, and MWs of **2-TIPS** and **2-TES** were both formed as suspensions. As shown in Figure 3a, **2-TIPS** formed “microbelts” (Figure S7, Supporting Information) hundreds of micrometers long; in contrast, **2-TES** formed “microwires” with a relatively high regularity in width ($2.72 \pm 0.72 \mu\text{m}$) (Figure 3). To correlate the observed nanowires with the molecular single crystal structure, selected-area electron diffraction (SAED) and crystallographic packing calculation were performed. The diffraction patterns were

(6) Coropceanu, V.; Jérôme, C.; da Silva Filho, D. A.; Olivier, Y.; Silbey, R.; Brédas, J.-L. *Chem. Rev.* **2007**, *107*, 926.

(7) (a) Tang, Q.; Jiang, L.; Tong, Y.; Li, H.; Liu, Y.; Wang, Z.; Hu, W.; Liu, Y.; Zhu, D. *Adv. Mater.* **2008**, *20*, 2947. (b) Zang, L.; Che, Y.; Moore, J. S. *Acc. Chem. Res.* **2008**, *41*, 1596.

(8) (a) Mas-Torrent, M.; Durkut, M.; Hadley, P.; Ribas, X.; Rovira, C. *J. Am. Chem. Soc.* **2004**, *126*, 984. (b) Tang, Q.; Li, H.; He, M.; Hu, W.; Liu, C.; Chen, K.; Wang, C.; Liu, Y.; Zhu, D. *Adv. Mater.* **2006**, *18*, 65. (c) Tang, Q.; Li, H.; Liu, Y.; Hu, W. *J. Am. Chem. Soc.* **2006**, *128*, 14634. (d) Tang, Q.; Li, H.; Song, Y.; Xu, W.; Hu, W.; Jiang, L.; Liu, Y.; Wang, X.; Zhu, D. *Adv. Mater.* **2006**, *18*, 3010. (e) Xiao, S.; Tang, J.; Beetz, T.; Guo, X.; Tremblay, N.; Siegrist, T.; Zhu, Y.; Steigerwald, M.; Nuckolls, C. *J. Am. Chem. Soc.* **2006**, *128*, 10700. (f) Briseno, A. L.; Mannsfeld, S. C. B.; Lu, X.; Xiong, Y.; Jenekhe, S. A.; Bao, Z.; Xia, Y. *Nano Lett.* **2007**, *7*, 668. (g) Zhou, Y.; Liu, W.; Ma, Y.; Wang, H.; Qi, L.; Cao, Y.; Wang, J.; Pei, J. *J. Am. Chem. Soc.* **2007**, *129*, 12386. (h) Kim, D. H.; Lee, D. Y.; Lee, H. S.; Lee, W. H.; Kim, Y. H.; Han, J. I.; Cho, K. *Adv. Mater.* **2007**, *19*, 678. (i) Zhou, Y.; Lei, T.; Wang, L.; Pei, J.; Cao, Y.; Wang, J. *Adv. Mater.* **2010**, *22*, 1484.

(9) Oh, J. H.; Lee, H. W.; Mannsfeld, S.; Stoltenberg, R. M.; Jung, E.; Jin, Y. W.; Kim, J. M.; Yoo, J.-B.; Bao, Z. *Proc. Natl. Acad. Sci. U.S.A.* **2009**, *106*, 6065.

indexed according to the single crystal data. For **2-TES**, the strong diffraction of (100), (020), and (040) was determined according to the single crystal data, which indicated that the single crystal nanowire were grown along the (100) direction. These results are in agreement with the Wulff plot of the crystal shape (Figure 3d) that was calculated using the Bravais-Fredel-Donnay-Harker (BFDH) method.¹⁰ Similar results were also obtained for **2-TIPS** and shown in Figure S7 (Supporting Information). As shown by the Wulff plots, the growing direction of the two nanowires is consistent with the column direction, which is the π - π stacking direction.

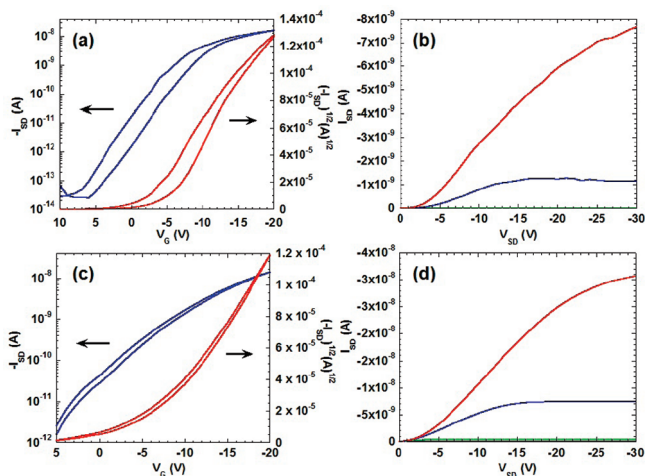


Figure 4. (a, c) Transfer and (b, d) output curves of the FET devices fabricated from (a, b) **2-TIPS** and (c, d) **2-TES** micro wires.

We also employed these MWs to fabricate the OFET devices. Single organic microwire transistors were fabricated by directly spin-coating the suspensions of the microwires onto the *n*-octadecyltrimethoxysilane (OTS)-treated $\text{SiO}_2/\text{n}^{++}\text{-Si}$ substrate. The OTS self-assembled monolayer (SAM) was modified according to the method reported by Bao and co-workers.¹¹ The polyethylene (PE) fibers with 20 μm diameter as a shadow mask were mounted on the wafer, and a gold layer with a thickness of 80 nm was deposited onto the substrate by thermal evaporation with the rate of 0.05 \AA s^{-1} . Devices fabricated using **1-TIPS** and **1-TES** as the active materials did not show obvious field-effect properties; this might be attributed to their unsuitable crystal packing. Both **2-TIPS** and **2-TES** molecules owned identical optical and electrochemical properties and even had similar crystal packing; however, they showed very different device performances. The transfer and output curves of both molecules are shown in Figure 4. Both **2-TIPS** and **2-TES** showed typical p-type charge-transport characteristics. **2-TIPS** exhibited a hole mobility up to $0.4 \text{ cm}^2 \text{ V}^{-1} \text{ s}^{-1}$ (average $0.15 \text{ cm}^2 \text{ V}^{-1} \text{ s}^{-1}$ from

(10) Donnay, J. D. H.; Harker, D. *Am. Mineral.* **1937**, *22*, 463. Calculation details are described in the Supporting Information.

(11) Ito, Y.; Virkar, A. A.; Mannsfeld, S.; Oh, J. H.; Toney, M.; Locklin, J.; Bao, Z. *J. Am. Chem. Soc.* **2009**, *131*, 9396.

20 devices), but **2-TES** only had a hole mobility of $0.05 \text{ cm}^2 \text{ V}^{-1} \text{ s}^{-1}$ (average $0.028 \text{ cm}^2 \text{ V}^{-1} \text{ s}^{-1}$ from 20 devices), which was an order of magnitude lower.

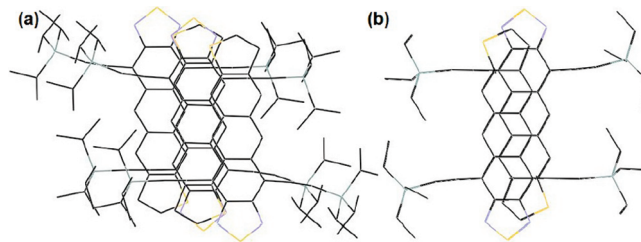


Figure 5. Intracolumn packing of (a) **2-TIPS** and (b) **2-TES** crystals.

A first-principle calculation based on the hopping model was employed to estimate the hole and electron mobility of **1-TIPS** and **1-TES** (Supporting Information).^{6,12} The computational results show that the main transporting channels of hole or electron were along the column. The hole mobility was estimated to be $1.23 \text{ cm}^2 \text{ V}^{-1} \text{ s}^{-1}$ for **2-TIPS** and $0.02 \text{ cm}^2 \text{ V}^{-1} \text{ s}^{-1}$ for **2-TES**, which is consistent with our experimental results. This large difference of the hole mobility can be attributed to the different intracolumn packings. As shown in Figure 5, **2-TIPS** has two types of intermolecular distances and overlaps, and **2-TES** has only one intermolecular distance and overlap in the column. In addition, the electron mobilities of **2-TIPS** and **2-TES** were also calculated and up to 0.65 and $1.28 \text{ cm}^2 \text{ V}^{-1} \text{ s}^{-1}$, respectively. However, we did not observe the electron transport in the nanowires, which may be attributed to oxygen trapping or injection barrier.¹³

In summary, we have developed a series of [2,1,3]thiadiazole-based oligoacenes **1-TES**, **1-TIPS**, **2-TES**, and **2-TIPS** through facile and convergent preparations. Such an approach provides a convenient route to develop various thiadiazole-fused oligoacene derivatives. These molecules exhibit unique crystal packing, largely different from other pentacene derivatives. The good performance with a hole mobility up to $0.4 \text{ cm}^2 \text{ V}^{-1} \text{ s}^{-1}$ is achieved from **2-TIPS**, which is quite high among the donor-acceptor pentacene derivatives. Theoretical prediction and OFET performances demonstrate that [2,1,3]thiadiazole-based oligoacenes are very promising for organic semiconducting materials.

Acknowledgment. This work was supported by the Major State Basic Research Development Program (No. 2009CB623601) from MOST and fundings from NSFC.

Supporting Information Available. Experimental details and ^1H and ^{13}C NMR spectra. This material is available free of charge via the Internet at <http://pubs.acs.org>.

(12) (a) Valeev, E. F.; Coropceanu, V.; da Silva Filho, D. A.; Salmeron, S.; Brédas, J.-L. *J. Am. Chem. Soc.* **2006**, *128*, 9882. (b) Wang, L.; Nan, G.; Yang, X.; Peng, Q.; Li, Q.; Shuai, Z. *Chem. Soc. Rev.* **2010**, *39*, 423.

(13) (a) Jung, B. J.; Tremblay, N. J.; Yeh, M.-L.; Katz, H. E. *Chem. Mater.* **2011**, *23*, 568. (b) Anthony, J. E.; Facchetti, A.; Heeney, M.; Marder, S. R.; Zhan, X. *Adv. Mater.* **2010**, *22*, 3876.